SURVEY OF LOCALIZED SOLAR FLARE SIGNATURES IN THE IONOSPHERE WITH GNSS, VLF, AND GOES OBSERVATIONS

IN43C-0092

Sandra Blevins (sandra.blevins@nasa.gov) [1], Laura Hayes [2], Yaireska Collado-Vega [3], Patrick Michael [3, 4], Carey Noll [3,4]

[1] Science Systems and Applications, Inc. (SSAI), Lanham, MD, USA; [2] Trinity College Dublin, Ireland; [3] NASA Goddard Space Flight Center (GSFC), Greenbelt, MD, USA; [4] Crustal Dynamics Data Information System (CDDIS), NASA GSFC

1 Introduction

Global navigation satellite system (GNSS) phase measurements of the total electron content (TEC) and ionospheric delay are sensitive to sudden increases in electron density in the layers of the Earth's ionosphere. These sudden ionospheric disruptions, or SIDs, are due to enhanced X-ray and extreme ultraviolet radiation from a solar flare that drastically increases the electron density in localized regions. SIDs are solar flare signatures in the Earth's ionosphere and can be observed with very low frequency (VLF ~ 3-30 kHz) monitors and dual-frequency GNSS (L1 = 1575.42 MHz, L2 = 1227.60 MHz) receivers that probe lower (D-region) to upper (F-region) ionospheric layers, respectively.

Figure 1: Earth's ionosphere is ionized by radiation from the Sun; here the ionospheric layers are illustrated during both night (left) and day (right)

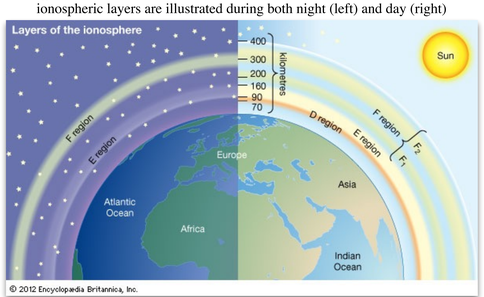

2 Data

Data from over 500 solar flare events, spanning April 2010 to July 2017, including GOES C-, M-, and X-class solar flares at various intensities, were collected from the Space Weather Database Of Notifications, Knowledge, Information (DONKI) developed at the NASA Goddard Space Flight Center (GSFC) Community Coordinated Modeling Center (CCMC). Historical GOES satellite (NOAA) X-ray flux (NASA GSFC CCMC integrated Space Weather Analysis system (iSWA)), and VLF SID (Stanford University Solar SID Space Weather Monitor program) time series data are available for all solar flare events of the sample set.

The GNSS daily data archived at the NASA GSFC Crustal Dynamics Data Information System (CDDIS) are used to characterize F-region reactions to increased ionization, complementing ground-based D-region (VLF) and space-based X-ray observations (GOES). CDDIS provides GNSS data with continuous 24-hour coverage from multiple satellites, at a temporal resolution of 30 seconds from over 400 stations.

3 Poster summary

For this poster we present a case study of one, strong solar flare event - the X6.9 class solar flare that occurred August 9, 2011 around 08:05 UTC. CDDIS data with continuous coverage from 100 unique GNSS receiver stations, spanning 20 countries at a variety of geographic locations are extracted and analyzed for signatures indicating flare detection. The geographic distribution of receivers enables us to explore the effects of this solar flare intensity at localized regions in Earth's ionosphere around the globe. The GNSS observations are combined with VLF SID and GOES data to characterize the unique multi-frequency signatures found, and to explore the impact of this strong solar flare event through the upper and lower layers of the Earth's ionosphere.

Trinity College Dublin
The University of Dublin

SSAI 40 Years Science Systems and Applications, Inc.

References

1 *Global Positioning System: Signals, Measurements, and Performances 2nd Edition*, Misra & Enge 2006

2 *Understanding GPS: Principles and Applications 2nd Edition*, Kaplan & Hegarty, 2006

4 GOES X-ray (Space)

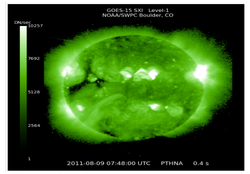

X6.9 class solar flare
Start time: 07:48 UTC
Peak time: 08:05 UTC
End time: 08:08 UTC
Source location: N17W69
Active region number: 11263

Figure 2: GOES-15 Solar X-ray Imager (SXI) capturing the active Sun at the event start time; the heat bar displays the data number (DN or discretized charge per pixel) per second (NOAA SWPC Boulder, CO; courtesy of NASA iSWA)

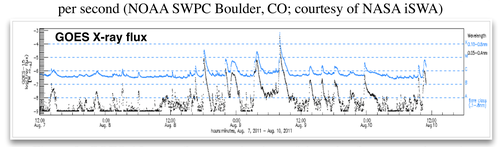

Figure 3: GOES-15 x-ray flux over the time of the solar flare event shown in black (wavelength range = 0.05 - 0.4 nm) and blue (wavelength range = 0.1 - 0.8 nm); the dashed horizontal lines measure flare class (plot from CCMC iSWA)

5 VLF SID (D-region)

Very low frequency (VLF) wave transmitters and receivers are used to probe levels of ionization in the lower, D-region of Earth's ionosphere by monitoring changes in signal strength due to sudden ionospheric disturbances (SIDs) from the enhanced x-ray and extreme ultraviolet radiation of solar flares.

Figure 4 (right) is an illustration of VLF signals bouncing off the D-region. Increasing ionization decreases VLF signal transmission through the ionosphere and the resulting signal strength as the waves are reflected and received by SID monitors.

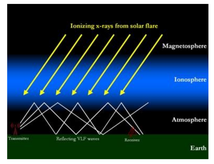

Figure 4: Very low frequency (VLF) wave diagram illustrating signals bouncing off the ionosphere D-region (Stanford University)

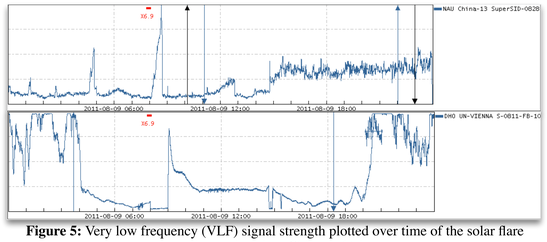

Figure 5: Very low frequency (VLF) signal strength plotted over time of the solar flare event in two location: China and Vienna

Figure 5 (above): VLF data obtained with sudden ionospheric monitors located in China (top) and Vienna (bottom). The signal magnitude is plotted over time in each figure, where the upwards and downwards facing arrows mark the time of sunrise and sunset for the monitors and stations (blue and black arrows, respectively; data courtesy of Stanford University's Solar Center). The small, red rectangle at the top of each subplot marks "X6.9", the start time of the solar flare event for this case study (07:48 UTC).

A variety of interesting signal features are present in each subplot. Prominent features present at the start of, and during the solar flare peak time of 08:05 may indicate sudden increases in ionization in the D-region, due to sudden x-ray and UV radiation from the solar flare.

6 GNSS (F-region)

A GNSS data extraction script, written in Python, was developed at the CDDIS to read RINEX version 2.11 o-files and extract observations, reported every 30 seconds, spanning 24 hours per each GNSS satellite with coverage available at the given epoch. Extracted data from 100 unique global GNSS receiver stations were analyzed using dual-frequency carrier phase (L1, L2; full cycles) and pseudorange code (P1, P2; meters) observables to estimate the ionospheric phase advance, group delay, and signal-to-noise ratios for all satellites present in the observations, over all epochs.

Figure 6 shows the carrier phase estimates of ionospheric delay for seven stations in different countries. In each subplot a weak peak, or delay pulse, is present in within the solar flare event time frame.

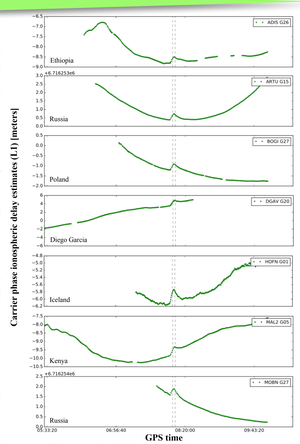

Figure 6: GPS carrier phase estimates of ionospheric delay plotted with time; the solar flare event marked by the two dashed lines

Left-hand subplots in Figure 7 (below) illustrate the pulse feature discovered in the LEIJ (Germany) carrier phase observations on the day of the X6.9 class solar flare (August 9, 2011), while the subplots on the right (below) from the same satellite and receiving station, show no signs of the pulse on the day before the event (no documented solar flare events are present in NASA GSFC DONKI on August 8, 2011).

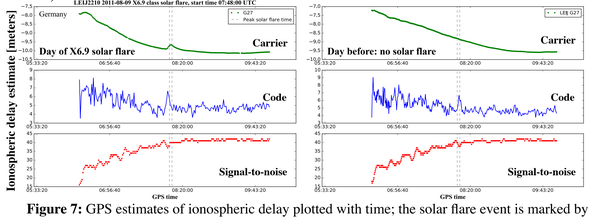

Figure 7: GPS estimates of ionospheric delay plotted with time; the solar flare event is marked by two dashed lines; characteristically smooth carrier phase advance (green) data are plotted on top, followed by noisy pseudorange code delay (blue) in the middle, and receiver-dependent signal-to-noise (red) at the bottom; the total system pseudorange error budget includes the space, control, and user segments with standard deviation values of 7.1 m [2]

7 Results

The ionospheric delay "pulse" was discovered in 36% of the case study GNSS observation files (o-files), appearing precisely at the time of the solar flare event, 08:05 - 08:08 UTC. The pulse appears for GPS satellites only; none appear to be present in GLONASS satellite observations. Specific GPS satellites will pick up the pulse feature (namely G15, G27, G8, and G9, among others). For example, pulse features were discovered in 58% of GNSS o-files for G15 satellite observations, specifically.

The number of individual satellite observations in o-files with delay pulses present are found to be higher in specific global regions. Figure 8 (right) shows the number of unique satellites in observation files with a delay pulse present by country.

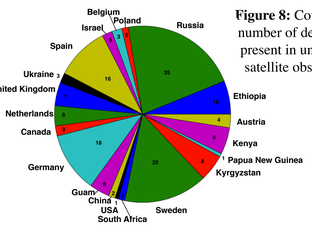

Figure 8: Countries and number of delay pulses present in unique GPS satellite observations

8 Conclusion

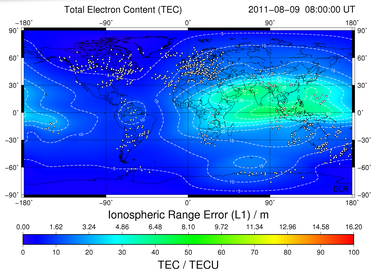

Figure 9: Total electron content (TEC) map for August 09, 2011 at 08:00 UTC provided by SWACI*; dashed contour lines mark the TEC in units of TECU (1 x 10^{16}) electrons per square meter; color bar scale indicates the ionospheric range error measured at frequency L1 (1575.42 MHz).

Figure 9 (above) displays regions of higher TEC densities which indicate higher levels of ionization occurring in the ionosphere at the time of the flare event. GPS signals propagating through these localized regions experience an increased delay due to higher electron densities caused by enhanced x-ray and extreme UV radiation from the solar flare. GNSS receiving stations with delay pulses present in observations are plotted as green stars, and stations without pulses are plotted as red circles, in Figure 10 (below). This figure illustrates that pulse feature occurrences correspond with global regions of higher TEC as compared with Figure 9.

Future work will include expanding the methods presented for this case study to GNSS satellite observations with simultaneous coverage for over 500 solar flare events of different strengths. Useful GNSS data metrics such as ionospheric delay, TEC, number of satellites, satellite observing angle, positions, receiving station latitude and longitude, and others will be made available to the community at the CDDIS archive. A statistical study will be conducted using these captured metrics to characterize the distribution of increased ionization due to various solar flare strengths, and use multi-frequency flare signatures to investigate the predicability of local and global regions that may be impacted by the different solar flare events in the sample.

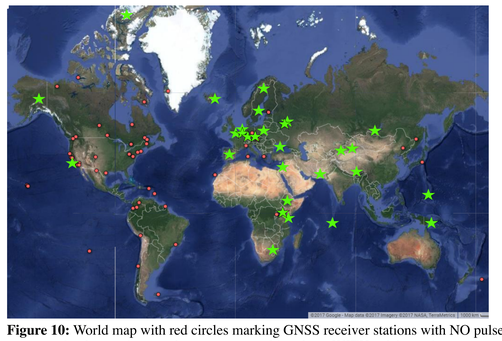

Figure 10: World map with red circles marking GNSS receiver stations with NO pulse present in observations, and green stars marking those WITH a delay pulse present

9 Acknowledgements

1 Trinity College Dublin

2 Space Weather Monitors at Stanford SOLAR Center, Stanford University

3 *Space Weather Application Center - Ionosphere (SWACI) of the German Aerospace Center eV. (DLR) in Neustrelitz, German

4 Community Coordinated Modeling Center (CCMC) at NASA GSFC Database Of Notifications, Knowledge, Information (DONKI)

5 Community Coordinated Modeling Center (CCMC) at NASA GSFC iNtegrated Space Weather Analysis tool (iSWA)